Effects of a mid-latitude solar eclipse on the thermosphere and ionosphere: a modelling study

Article

Published Version

It is advisable to refer to the publisher's version if you intend to cite from the work. See Guidance on citing.

www.reading.ac.uk/centaur

CentAUR

Central Archive at the University of Reading

Reading's research outputs online

Effects of a Mid-Latitude Solar Eclipse on the Thermosphere and Ionosphere - A Modelling Study

I.C.F. Müller-Wodarg, A. D. Aylward

Atmospheric Physics Laboratory, Department of Physics and Astronomy, University College London

M. Lockwood

Space Science Department, Rutherford Appleton Laboratory

Abstract. A modelling study is presented which investigates in-situ generated changes of the thermosphere and ionosphere during a solar eclipse. Neutral temperatures are expected to drop by up to $40°$ K at 240 km height in the totality footprint, with neutral winds of up to 26 m/s responding to the change of pressure. Both temperatures and winds are found to respond with a time lag of 30 min after the passing of the Moon's shadow. A gravity wave is generated in the neutral atmosphere and propagates into the opposite hemisphere at around 300 m/s. The combined effects of thermal cooling and downwelling lead to an overall increase in [O], while $[N_2]$ initially rises and then for several hours after the eclipse is below the "steady state" level. An enhancement of [NmF2] is found and explained by the atmosphere's contraction during, and the reduced $[O]/[N_2]$ ratio after the eclipse.

Introduction

The following study investigates the effects of a solar eclipse on the upper atmosphere, using the Coupled Thermosphere- Ionosphere-Plasmasphere Model (CTIP). We investigate the forthcoming solar eclipse of August 11, 1999, with a path of totality starting at 9:32 Universal Time (UT) near $41.0°$ N/$65.1°$ W, south of Nova Scotia. The moon's shadow will move across the south- western corner of the U.K. mainland at 10:10 UT and continue across central France (10:20 UT), southern Germany (10:30 UT), Austria (10:40 UT), Hungary (10:50 UT), Romania (11:00 UT), central Turkey (11:20 UT) and disappear near the Bay of Bengal ($20.6°$ N, $77.5°$ E) at 12:34 UT.

Previous studies of effects in the upper atmosphere caused by solar eclipses include those by *Singh et al.,* [1989] and *Cheng et al.,* [1992]. *Fritts and Luo* [1993] investigated the generation of gravity waves in the middle atmosphere during solar eclipses. These studies discuss observations exclusively on the assumption that a solar eclipse reduces ozone heating in the middle atmosphere. It is thus of interest to investigate how far a reduction of in-situ thermospheric and ionospheric solar absorption might contribute to eclipse effects in the upper atmosphere. *Roble et al.,* [1986] carried out an equivalent simulation with the NCAR Thermosphere General Circulation Model (TGCM), but did not include a fully coupled ionosphere.

The CTIP Model

The Coupled Thermosphere-Ionosphere- Plasmasphere Model (CTIP) [*Fuller-Rowell et al.*, 1996; *Millward et al.*, 1996, and references therein] solves self-consistently the time-dependent, 3-D coupled equations of momentum, energy and continuity for neutral particles and ions. Thermospheric calculations are carried out on a spherical co-rotating pressure coordinate grid with spacings of $2°$ in latitude, $18°$ in longitude and one scale height vertically, between 80 km and around 450 km altitude, at time steps of 60 seconds. The ionosphere uses a spherical height coordinate system with the same horizontal resolution, but height levels ranging from 100 to around 10000 km.

To consider the moon's shadow, the solar heating function was set to zero in a footprint moving at the appropriate velocity (on average 1.5 km/s) along the path of totality. The large region of half-shadow was also considered, assuming an increase of solar luminosity by 3 % of the non-eclipsed value per 100 km distance from the totality footprint. The simulation was carried out for August 11, 1999, assuming a solar F10.7 flux index of 190 and magnetic activity index of Kp=2+. In order to identify the effects of the eclipse, a further simulation was run for identical conditions, but excluding the eclipse shadow.

Results and Discussion

Results presented in the following are differences between the eclipse and non-eclipse simulation, with positive (negative) values denoting an increase (decrease) of the parameter in the eclipse simulation.

Thermospheric changes

Figure 1 shows changes of neutral temperature (solid line) and horizontal winds (dashed: northward; dotted: eastward) at 240 km altitude for latitudes $30°$ N, $50°$ N and $70°$ N, corresponding to locations south of, at and north of the totality footprint at that particular UT (11:30): the peak temperature decrease is of around $30°$ K, $45°$ K and $20°$ K, respectively, at these latitudes, corresponding to around 2.5 %, 3.8 % and 1.7 % of the average background temperature ($1200°$ K). The reduction in temperature causes a decrease of pressure over the totality footprint to which the neutral winds respond. At $30°$ N, the eclipse generates northward winds reaching 25 m/s, while at $70°$N they are southward, reaching 15 m/s. Zonal wind changes are below 10 m/s at $30°$ N and reach 20 m/s at $70°$ N. Considering that typical wind speeds found by the CTIP for these latitudes are up to
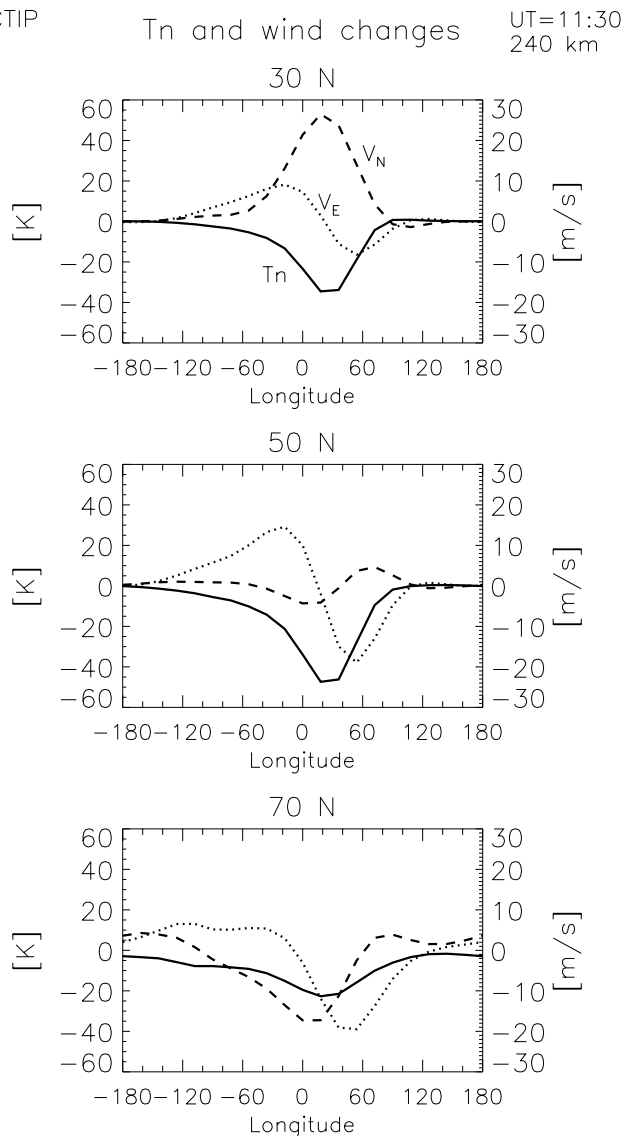
Figure 1. The changes of neutral temperature and winds at 11:30 UT for 240 km altitude and 3 different latitudes, as predicted by the CTIP for the August 11, 1999 solar eclipse. Solid lines denote temperature, dashed and dotted lines northward- and eastward wind components, respectively.

around 100 m/s, these eclipsed-induced changes in neutral winds are important. When producing a global snapshot of wind changes (not shown) one sees an anticlockwise flow around the low pressure region. Ion drag plays a minor role since the footprint of totality is far from the magnetic pole and auroral oval, and the flow is thus to a reasonable approximation geostrophic. The patterns of neutral temperature and wind changes agree well with those found by *Roble et al.,* [1986] for the May 30, 1984 eclipse. Any discrepancies can be explained through the differences in the paths, with the 1984 eclipse occurring at lower latitudes, giving a weaker Coriolis force acting on the neutral winds.

Figure 2 shows the change of temperature at longitude 0° as a function of UT and latitude. The plot shows that the peak temperature decrease occurs at around 10:50 UT.

However, the centre of the moon's shadow crosses this longitude at around 10:20 UT, so it is evident that there is a time lag of around 30 minutes between the totality and the peak temperature decrease; winds respond with the same time lag. A further interesting feature of Figure 2 is the global propagation of the temperature disturbance. One sees that the change of temperature is strongest at 50° N, where the path of totality crosses the longitude 0° meridian. In addition, two wavefronts are formed, one propagating over the north pole to the opposite longitude (not shown) and the other equatorward into the southern hemisphere. The wave velocity is of around 300 m/s and agrees well with values measured by *Singh et al.,* [1989]. Although magnitudes of most temperature changes are not measureable with any of today's instruments it must be emphasized that the values presented here are a result of reduced in-situ absorption in the upper atmosphere only. This issue is discussed further in section 4.

Ionospheric and Neutral Composition changes

Changes occurring near the F2 peak altitudes at latitude 50° N and longitude 0° are shown in Figure 3. The graphs are the changes of the F2 peak electron density ([NmF2], solid line) and of N_2 and O densities (dashed and dotted lines, respectively) on the pressure level closest to the F2 peak height. The beginning ("first contact" at 9:50 UT) and end ("fourth contact" at 11:16 UT) of the eclipse are marked by vertical bars. The following will discuss the neutral composition changes and outline how these may affect the electron densities. Although Figure 3 shows one particular location only, the behaviour was found to be similar for others along the path of totality.

One sees from Figure 3 that N_2 densities increase during the first half of the eclipse by up to around $3 \cdot 10^{13} m^{-3}$, or around 5 %, then fall again and become smaller than the "steady state" values for around 10 hours after the eclipse, by up to $2 \cdot 10^{13} m^{-3}$, or 3 %. The behaviour of the O densities is different in that they stay larger than the "steady state" values throughout the eclipse and for around 14 hours afterwards. Their largest increase occurs at around 11:30 UT, reaching around $7 \cdot 10^{13} m^{-3}$, or 5 % of the background value.

As a result of the falling temperature, one would expect densities on a level of fixed pressure to rise. It was shown earlier (see Figure 2) that the peak temperature decrease occurs around 30 minutes after totality, or 10:50 UT. Although it was there shown for a fixed altitude, the temperature behaviour on a fixed pressure level was found to be very similar. If cooling were the only process influencing densities, the curves of [O] and [N_2] in Figure 3 should fall after 10:50 UT, due to the temperature rise after totality. However, the N_2 density already begins to fall before that, at 10:30 and [O] begins to fall only at 11:30 UT. So cooling alone cannot account for the observed behaviour.

Another important process is the downwelling, or downward transport of gases. Downwelling is a result of the converging horizontal winds which surround the eclipsed region and cause a downward flux relative to pressure levels in order to conserve mass [*Rishbeth et al.,* 1969]. Cooling itself, without the downwelling, would cause no real composition change on a fixed pressure level, so the relative concentrations of gas components would remain unchanged [*Rishbeth and Müller-Wodarg,* 1999]. The downwelling, however, does
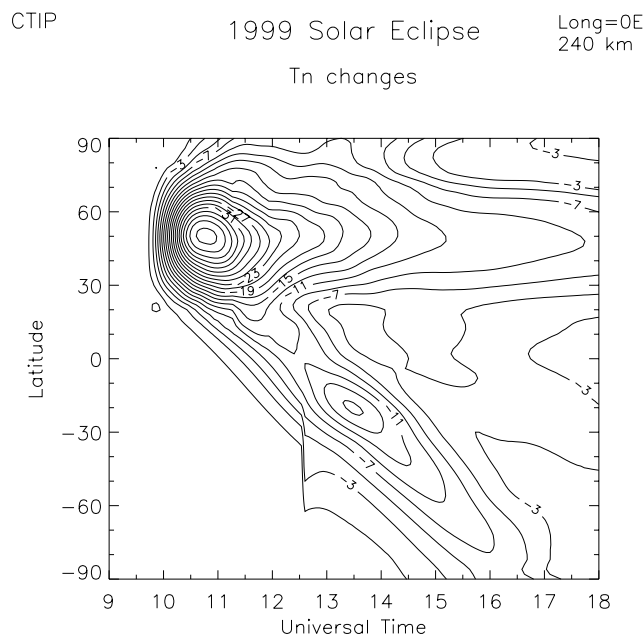
Figure 2. Temperature changes during the August 11, 1999 solar eclipse at longitude $0°$ for 240 km altitude.

change the composition since air from higher pressure levels with different relative gas concentrations is transported downwards. One sees in Figure 3 that densities of O and N_2 increase during the first half of the eclipse, between 9:50 UT and around 10:20 UT. As shown above, these density increases are consistent with the cooling. When plotting the change of the $[O]/[N_2]$ ratio (not shown) one will however see that the relative concentration of O increases, which is what one would expect from the downwelling, carrying [O]-rich gases from higher to lower pressure levels. This shows that both processes, cooling and downwelling, play a role here. The downwelling will upset diffusive balance, so molecular diffusion will act to restore the equilibrium. Molecular diffusion is thus the third process determining neutral gas densities in Figure 3.

When discussing the $[N_2]$ behaviour, it is important to note that cooling and downwelling have competing effects on its concentration: while cooling leads to an increase of $[N_2]$, downwelling decreases it. As a result of the cooling, $[N_2]$ rises between 9:50 and 10:20 UT. After that, downwelling has become strong enough to dominate effects of the cooling and the N_2 concentration begins to drop. As temperature increases again, after 10:50 UT, the atmosphere expands and further reduces the densities. As a result of both the downwelling and expansion, $[N_2]$ drops below the steady state level after 11:20 UT. Molecular diffusion of N_2 into the previously eclipsed region eventually leads to an overall rise of $[N_2]$ after 14:30.

The combined effects of downwelling and cooling lead to a sharp rise of [O] after 9:50 UT. After the temperature minimum at 10:50 UT, the O density in Figure 3 still increases for some time (due to the downwelling), but at a reduced rate (due to the heating), maximizing at 11:30 and then falling. The continuous decrease of [O] after 11:30 is a result of the atmosphere's expansion and molecular diffusion.

In Figure 3, [NmF2] (solid line) increases during the eclipse by up to $4 \cdot 10^{10} m^{-3}$, or 8 % of the background

value, corresponding to a change in the F2 layer critical frequency, f_oF2, by around 0.2 MHz. These changes are very small and hardly measurable, but nevertheless it is of interest to discuss what causes them. Some of this [NmF2] behaviour is due to the atmosphere's contraction and some can be explained from the neutral composition changes. It is well known that daytime F2 region electron densities are sensitive to neutral composition: production depends on the O concentration, while the loss rate depends on mainly the N_2 concentration. As a rule of thumb, daytime [NmF2] increases with the $[O]/[N_2]$ ratio. During the eclipse, no photoionization of O occurs, so the O density is irrelevant. It was found earlier that N_2 densities increase during the eclipse, which should lead to a decrease of [NmF2]. As with the neutral densities, though, the atmosphere's compression (due to cooling) also causes an increase in electron densities on a fixed plasma pressure level. So, the two processes ("thermal increase" and "chemical reduction") compete against each other.

The fastest reaction leading to recombination of ions and electrons is via N_2 and $NO+$, and reaction rate calculation reveal that an increase in $[N_2]$ by 5 % would over 30 minutes lead to a reduction of [NmF2] by around 1 %. So, the "chemical reduction" is too weak to cause an overall decrease of $[N_2]$ in Figure 3.

Initially, after the temperature minimum at 10:50 UT, [NmF2] does fall again as a result of the thermal expansion. About an hour later, though, photoionization under the enhanced $[O]/[N_2]$ ratio causes an overall increase in [NmF2] to its second maximum, at around 13:30. The slow decrease of $[O]/[N_2]$ (due to molecular diffusion) during the afternoon hours then causes the observed reduction of [NmF2]. In summary, the initial increase of [NmF2] is a result of the atmosphere's compression, while the behaviour after the eclipse is linked to the neutral composition.

Similar to the earlier findings about temperature perturbations, the electron density changes propagate as a wave away from the path of totality (not shown here). However, disturbances propagate into the equatorial regions only and
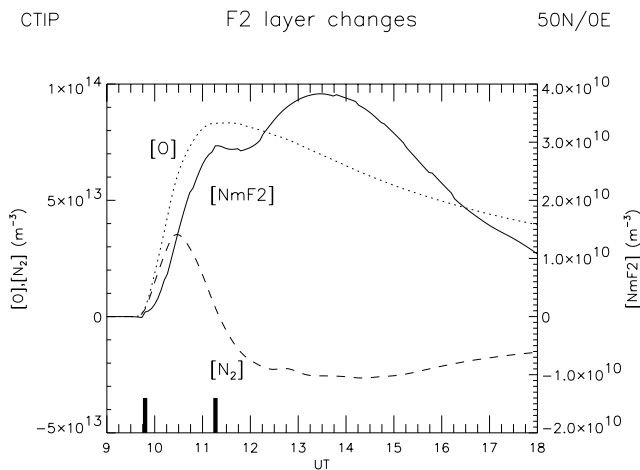
Figure 3. Changes of parameters at and near the F2 peak height during the August 11, 1999 solar eclipse at latitude $50°$ N and longitude $0°$. The panel shows [NmF2] (solid) as well as O (dotted) and N_2 densities (dashed) at the pressure level closest to the F2 peak. All densities are given in $[m^{-3}]$.

not across the north pole. The high-latitude electric field and auroral oval destroy any eclipse-driven ionospheric disturbances.

Conclusions and possible limitations

The above findings provide a morphological insight into processes occurring in the thermosphere and ionosphere as a result of a temporary reduction in the flux of heating and ionizing radiation. It is of interest to discuss where possible limitations of the simulations may lie in relation to solar eclipses.

As mentioned previously, the presented simulations do not consider any eclipse contribution from the middle atmosphere, where ozone absorption is strong, so effects associated with that will not be seen here. This has advantages in that one can clearly separate the contributions from below and in-situ. Overall, the only measurable changes found were in the neutral winds and composition. So, if measurements find a stronger response in the upper atmosphere during this or any other mid-latitude eclipse one may, following the results presented here, assume that these originate from outside the thermosphere-ionosphere system. Studies by *Fritts and Luo* [1993] suggest that perturbations generated by the interrupted ozone heating during an eclipse may propagate upwards into the thermosphere and have an important dynamical influence there. In a more extensive future study, their predicted global perturbation profile may be adapted for use at CTIP's lower boundary. In that way, eclipse disturbances originating from both below the thermosphere and from in-situ can be considered and their relative importance to the thermosphere/ionosphere system evaluated.

The simulations assumed geomagnetically quiet and constant conditions. In reality, the high-latitude precipitation and electric field strength vary randomly and may thus obscure some of the weaker effects.

No distinction was made in the CTIP simulation between various wavelength bands in that the intensity at all wavelengths was set to zero in the totality footprint. It is known that up to 10-20 % of the solar soft-X-ray and EUV radiation (< 100nm) originate from the solar corona, which is not darkened during an eclipse. As a result, these wavebands will not disappear entirely.

With the limitations noted, the simulations presented provide us with predictions of the major changes to the ionosphere-thermosphere system during the August 1999 eclipse and have provided an important basis for evaluating the viability of observations in the upper atmosphere during the event. The predictions and modelling are the most self-consistent yet made and any differences to the observations will provide valuable information, particularly on coupling to lower atmospheric layers.

References

Cheng, K., Y.-N. Huang, and S.-W. Chen, Ionospheric Effects of the Solar Eclipse of September 23, 1987, Around the Equatorial Anomaly Crest Region, *J. Geophys. Res., 97,* 103-111, 1992.

Fritts, D.C., and Z. Luo, Gravity Wave Forcing in the Middle Atmosphere Due to Reduced Ozone Heating During a Solar Eclipse, *J. Geophys. Res., 98,* 3011-3021, 1993.

Fuller-Rowell, T.J., D. Rees, S. Quegan, R.J. Moffett, M. V. Codrescu, and G. H. Millward, A Coupled Thermosphere-Ionosphere Model (CTIM), *Solar Terrestrial Energy Program (STEP) Handbook*, edited by R. W. Schunk, pp. 217-238, 1996.

Millward, G.H., R.J. Moffett, S. Quegan, and T.J. Fuller-Rowell, A Coupled Thermosphere-Ionosphere-Plasmasphere Model (CTIP), *Solar Terrestrial Energy Program (STEP) Handbook*, edited by R. W. Schunk, pp. 239-279, 1996.

Rishbeth, H., R. J. Moffett, and G. J. Bailey, Continuity of Air Motion in the Mid-Latitude Thermosphere, *J. Atmos. Terr. Phys., 31,* 1035-1047, 1969.

Rishbeth, H., and I.C.F. Müller-Wodarg, Vertical Circulation and Thermospheric Composition: A Modelling Study, *submitted to Ann. Geophys.*, 1999.

Roble, R.G., B. A. Emery, and E. C. Ridley, Ionospheric and Thermospheric Response over Millstone Hill to the May 30, 1994 Annual Solar Eclipse, *J. Geophys. Res., 91,* 1661-1670, 1986.

Singh, L., T. R. Tyagi, Y. V. Somayajulu, P. N. Vijayakumar, R. S. Dabas, B. Loganadham, S. Ramakrishna, P. V. S. Rama Rao, A. Dasgupta, G. Navneeth, J. A. Klobuchar, and G. H. Hartmann, A Multi-Station Satellite Radio Beacon Study of Ionospheric Variations During Total Solar Eclipses, *J. Atmos. Terr. Phys., 51,* 271-278, 1989.

I.C.F. Müller-Wodarg, Atmospheric Physics Laboratory, Department of Physics and Astronomy, University College London, 67-73 Riding House Street, London W1P 7PP, U.K. (e-mail: ingo@apg.ph.ucl.ac.uk)

A. D. Aylward, Atmospheric Physics Laboratory, Department of Physics and Astronomy, University College London, 67-73 Riding House Street, London W1P 7PP, U.K. (e-mail: alan@apg.ph.ucl.ac.uk)

M. Lockwood, Space Science Department, Rutherford Appleton Laboratory, Chilton, Didcot, Oxfordshire, OX11 0QX, U.K. (e-mail: m.lockwood@rl.ac.uk)